Journal of Organometallic Chemistry 907 (2020) 121064

Contents lists available at ScienceDirect

Journal of Organometallic Chemistry

journal homepage: www.elsevier.com/locate/jorganchem

Synthesis, characterization, and biological properties of rhenium(I) tricarbonyl complexes bearing nitrogen-donor ligands

Brendan L. Murphy [a], Sierra C. Marker [b], Valencia J. Lambert [c], Joshua J. Woods [b, d], Samantha N. MacMillan [b], Justin J. Wilson [b, *]

[a] Department of Radiology, Weill Cornell Medicine, New York, NY, 10065, United States
[b] Department of Chemistry and Chemical Biology, Cornell University, Ithaca, NY, 14853, United States
[c] College of Human Ecology, Cornell University, Ithaca, NY, 14853, United States
[d] Robert F. Smith School for Chemistry and Biomolecular Engineering, Cornell University, Ithaca, NY, 14853, United States

ARTICLE INFO

Article history:
Received 14 November 2019
Received in revised form
2 December 2019
Accepted 3 December 2019
Available online 5 December 2019

Keywords:
Rhenium
Photophysical properties
Anticancer agents
Metal-based drugs

ABSTRACT

Rhenium(I) tricarbonyl complexes have properties that make them valuable for various biomedical applications, such as imaging, cancer treatment, and bactericidal uses. The ability to modify the ligand coordination sphere of these complexes enables researchers to fine-tune and optimize their properties for biological use. In this study, we explored the role of axial nitrogen-donor ligands. Specifically, the compounds *fac*-$[Re(CO)_3(phen)(L)]^+$, where phen = 1,10-phenanthroline and L = pyridine (**Re-py**), piperidine (**Re-pip**), morpholine (**Re-morph**), and thiomorpholine (**Re-thio**), were synthesized and characterized. X-ray crystal structures of these complexes show that they obtain an expected pseudo-octahedral geometry with the three CO ligands arranged in a facial manner. Additionally, the X-ray crystal structure of a byproduct from these reactions, the hydroxo-bridged dinuclear Re compound $[(CO)_3(phen)Re(\mu\text{-}OH)Re(phen)(CO)_3]^+$, is described. The photophysical properties of these complexes were investigated in detail, revealing that they are photoluminescent in air-equilibrated pH 7.4 phosphate-buffered saline with quantum yields ranging from 1.7 to 3.1%. Both the quantum yields and emission energies were found to correlate with the basicity of the axial nitrogen donor, whereby more basic ligands give rise to smaller quantum yields and lower-energy emissions. These four compounds were further evaluated for their potential as fluorescence microscopy imaging agents. Of the four compounds, only **Re-py** showed detectable intracellular luminescence in HeLa cells. Lastly, the cytotoxicities of these compounds in HeLa cells were determined. None of the four compounds is significantly cytotoxic as reflected by their 50% growth inhibitory concentrations that exceed 30 μM.

© 2019 Elsevier B.V. All rights reserved.

1. Introduction

The highly stable rhenium(I) tricarbonyl, $Re(CO)_3$, structural motif has been explored for decades for its novel photophysical and catalytic properties [1,2]. It has been realized in recent years that these properties make such complexes appealing for biological applications as well. Most notably, these $Re(CO)_3$ complexes have found use as imaging agents and have shown promise for antibacterial and anticancer applications [3–9]. The synthetic ease by which these complexes can be modified via straightforward ligand substitution reactions has enabled researchers to access a diverse range of complexes with spectroscopic and biological properties tuned for different uses in biology.

$Re(CO)_3$ complexes bearing diimine ligands of the type $[Re(CO)_3(NN)(X/L)]^{0/1+}$, where NN is a diimine ligand and X and L are anionic or neutral axial ligands, typically possess the most favorable photophysical properties for biological imaging, by virtue of their luminescent metal-to-ligand charge transfer (MLCT) excited state [7,10–13]. Modifications to the diimine ligand can have a profound effect on both the photophysical and biological properties of the $Re(CO)_3$ complex by altering the energy of the accepting ligand-based π-orbitals, the rates of axial ligand substitution [14], and the overall complex lipophilicity. The nature of the axial ligand plays a subtler, albeit important, role in modulating these properties. The use of an appropriate axial ligand, for example, can yield complexes with enhanced photoluminescent

* Corresponding author.
E-mail address: jjw275@cornell.edu (J.J. Wilson).

https://doi.org/10.1016/j.jorganchem.2019.121064
0022-328X/© 2019 Elsevier B.V. All rights reserved.

quantum yields [1,2]. Additionally, certain ligands, such as phosphines, give rise to CO photosubstitution processes by exerting a strong trans influence in the excited state [15,16].

The types of axial nitrogen-donor ligands that have been employed on $Re(CO)_3$ complexes have been predominately limited to analogues of pyridine [17–30]. Thus, there remains a need to gain a more comprehensive understanding of the importance of this class of ligands for tuning the properties of these complexes. In this study, we aimed to explore the use of alternative nitrogen-donors to investigate the role of these ligands on the photophysical and biological properties of the resulting $Re(CO)_3$ complexes. We chose the nitrogen donors piperidine (pip), morpholine (morph), and thiomorpholine (thio) based on their differential donor strengths, which are reflected by their pK_a values that range from 5 to 11. To aid in comparative purposes, we used the simple diimine ligand 1,10-phenanthroline (phen) throughout. The photophysical and biological properties of these newly prepared compounds were then evaluated. This study adds to the growing interest in $Re(CO)_3$ complexes for use in biology and further elucidates how the properties of these compounds can be rationally modified by the appropriate ligand choice.

2. Results and discussion

2.1. Synthesis and characterization

The three $Re(CO)_3$ complexes *fac*-[$Re(CO)_3$(phen)(pip)]OTf (**Re-pip**), *fac*-[$Re(CO)_3$(phen)(morph)]OTf (**Re-morph**), and *fac*-[$Re(CO)_3$(phen)(thio)]OTf (**Re-thio**), where OTf = trifluoromethanesulfonate, were synthesized by treating *fac*-[$Re(CO)_3$(phen)Cl] with AgOTf in refluxing tetrahydrofuran (THF) to remove the axial chloride ligand as insoluble AgCl, followed by the addition of an excess of either pip, morph, or thio (Scheme 1). Although analytically pure **Re-morph** was obtained as a precipitate directly from the reaction mixture, **Re-pip** and **Re-thio** required additional purification via crystallization from THF. **Re-pip** has been previously reported, but its synthesis and characterization have not been described in detail [31]. For comparative purposes, the previously reported complex *fac*-[$Re(CO)_3$(phen)(py)]OTf (**Re-py**), where py = pyridine, was also prepared in a similar manner, and its characterization data are consistent with those in the literature [17,31]. **Re-pip**, **Re-morph**, and **Re-thio** were characterized by ^{1}H (Figs. S1–S3) and ^{19}F (Figs. S4–S6) NMR spectroscopy, IR spectroscopy (Figs. S7–S10), electrospray ionization mass spectrometry (ESI-MS, Figs. S11–S13), and single-crystal X-ray diffraction, and their purities were verified by elemental analysis and high-performance liquid chromatography (HPLC, Figs. S14–S16). Their ^{1}H NMR spectra show all of the expected resonances for these compounds. Notably, the axial and equatorial hydrogen nuclei of the pip, morph, and thio ligands are inequivalent, indicating that chair-chair interconversion of these six-membered cyclic donor ligands is slow on the NMR timescale at room temperature [32–34]. The ^{19}F NMR spectra of these complexes reveal a single resonance at −77 ppm, corresponding to the OTf^- counterion. IR spectroscopic analysis of these complexes reveals the presence of intense CO stretching modes in the range of 1890–1930 cm^{-1}. For **Re-pip**, **Re-thio**, and **Re-py** three distinct peaks corresponding to CO stretching modes are apparent. This result is consistent with their C_s symmetry, which will give rise to 3 IR-allowed transitions [35]. By contrast, the IR spectrum of **Re-morph** displayed an additional set of 3 CO stretching modes. Notably, all other characterization data of this complex support the conclusion that this complex is a single, pure species. Therefore, we hypothesize that the presence of additional CO stretching modes reflects the existence of two isomeric forms of this complex. Because the IR timescale is substantially faster than that of NMR spectroscopy, the fact that these putative isomers are observed by the former technique but not the latter suggests that they are interconverting rapidly ($>10^{12}$ s^{-1}) [36]. Such timescales may be afforded by isomers that would exist upon rotation of the morph ligand about the Re–N vector. For example, dynamic IR spectroscopy has been used to probe the fast isomeric interconversion of tricarbonyl(η^4-1,5-cyclooctadiene)iron(0) [36–38], in which the carbonyl ligands move between apical and basal sites on this complex via a turnstile-like mechanism.

2.2. X-ray crystallography

Single crystals were obtained for all four complexes, and their crystal structures were determined by X-ray crystallography. The structures are shown in Fig. 1, and selected interatomic distances and angles are collected in Table 1 and Table S2. All complexes attain the expected octahedral geometry for a low-spin d^6 metal center. Notably, the structures of both **Re-morph** and **Re-thio** show that the morph and thio ligands coordinate to the Re center through the nitrogen atoms rather than the oxygen or sulfur donors, respectively. The six-membered pip, morph, and thio ligands all attain a stable chair conformation, with the Re center occupying an equatorial site on the bound nitrogen. Despite the different pK_a values and donor strengths of the axial ligands, the Re–N_{axial} interatomic distances are invariant across the three complexes with distances between 2.246(3)–2.257(2) Å. For **Re-py**, however, this Re–N_{axial} interatomic distance is 2.216(2) Å, somewhat shorter than those for **Re-pip**, **Re-morph**, and **Re-thio**. This slightly shorter distance may be a consequence of the weak π-acceptor capabilities of py in contrast to the pure σ donors pip, morph, and thio. The lack

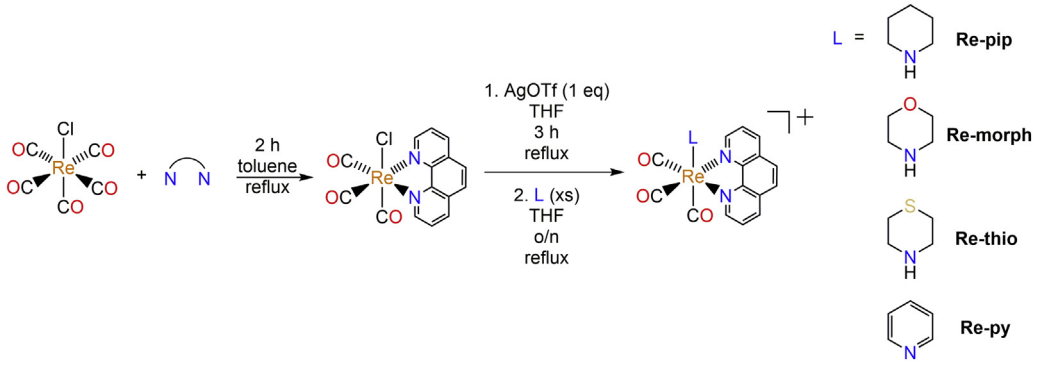

Scheme 1. Synthetic scheme for the preparation of *fac*-[$Re(CO)_3$(phen)(L)]$^+$ complexes.

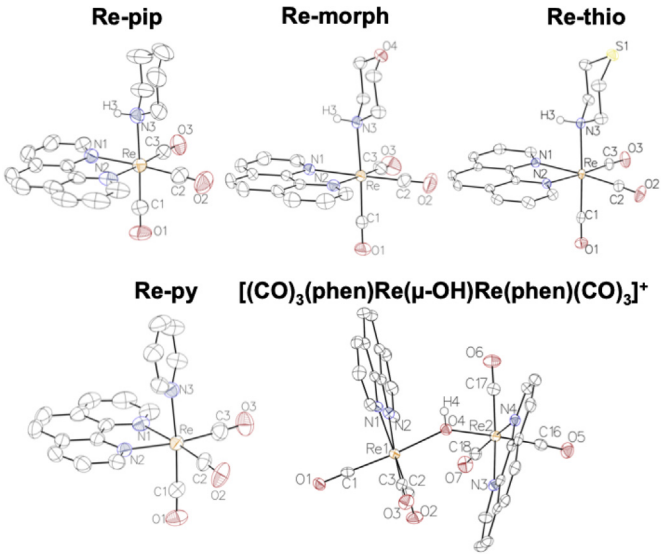

Fig. 1. X-ray crystal structures of **Re-pip**, **Re-morph**, **Re-thio**, **Re-py**, and [**(CO)$_3$(phen)Re(μ-OH)Re(phen)(CO)$_3$**]$^+$. Ellipsoids are drawn at 50% probability. Non-acidic hydrogen atoms and the counterions are omitted for clarity.

Table 1
Selected interatomic distances.[a]

Selected Interatomic Distances (Å)	Re-pip	Re-morph	Re-thio	Re-py
Re–N_1	2.182(2)	2.181(2)	2.181(2)	2.178(2)
Re–N_2	2.179(2)	2.175(2)	2.178(2)	2.170(2)
Re–N_3	2.246(3)	2.249(2)	2.257(2)	2.216(2)
Re–C_1	1.908(3)	1.922(3)	1.923(2)	1.918(3)
Re–C_2	1.915(3)	1.913(3)	1.927(2)	1.924(3)
Re–C_3	1.924(3)	1.923(3)	1.921(2)	1.919(3)

[a] Atoms are labeled as shown in Fig. 1. Numbers in parentheses are the estimated standard deviations for the last significant figure.

of variance in the axial ligand bond distances of **Re-pip**, **Re-morph**, and **Re-thio** suggests that the Re–N_{axial} interatomic separation is a poor metric for the donor strength of these axial ligands, which should be related to their pK_a values. The Re–$N_{equatorial}$ distances are similar among the four complexes with values ranging from 2.170(2)–2.182(2) Å. In comparison, the four complexes also exhibit similar Re–CO_{axial} and Re–$CO_{equatorial}$ interatomic distances of 1.908(3)–1.923(2) Å and 1.913(3)–1.927(2) Å, respectively. Lastly, all interatomic angles are relatively invariant between the four complexes.

While attempting to crystallize **Re-pip**, we serendipitously obtained and analyzed a crystal of the dirhenium μ-hydroxo species, [**(CO)$_3$(phen)Re(μ-OH)Re(phen)(CO)$_3$**]$^+$ (Fig. 1, Table S3). This complex cation and related analogues with 2,2′-bipyridine and 4,4′-dimethyl-2,2′-bipyridine ligands have previously been reported [39–43]. Although these complexes can be obtained in moderate yield from the reaction of [Re(CO)$_3$(NN)(OTf)] with KOH under anhydrous conditions, they have more often been isolated in low yields as reaction byproducts that arise from the presence of adventitious hydroxide [39]. The discovery of [**(CO)$_3$(phen)Re(μ-OH)Re(phen)(CO)$_3$**]$^+$ as an unintended byproduct in our synthesis of **Re-pip** is most likely a consequence of small amounts of water present in the THF solution that are deprotonated by the pip ligand. Our observation that this byproduct only arises from the reaction with pip is consistent with the fact that this ligand is the most basic of the axial nitrogen donors explored in this study.

The structure of [**(CO)$_3$(phen)Re(μ-OH)Re(phen)(CO)$_3$**]$^+$ reveals that the Re–(OH)–Re vector is bent with an angle of 133.18(13)°. For the related complexes [(CO)$_3$(NN)Re(μ-OH)Re(NN)(CO)$_3$]$^+$, where NN = 2,2′-bipyridine and 4,4′-dimethyl-2,2′-bipyridine, the Re–(OH)–Re angles range from 132.8(6)–140.50(7)° [39–42], and different polymorphs of the Br$^-$ salt of [**(CO)$_3$(phen)Re(μ-OH)Re(phen)(CO)$_3$**]$^+$ have Re–(OH)–Re angles that range from 130.90(7)–140.70(19)° [43]. These data indicate that this angle is highly dependent on the solid-state packing of this compound. Additionally, the bridging OH ligand within this compound class is known to form hydrogen bonds with acceptors in the crystal lattice [43]. In the structure reported here, a hydrogen bond between this bridging ligand and an acetonitrile solvent molecule is present, as characterized by a O–N distance of 3.043(5) Å (Fig. S17). The distance between the Re centers and the bridging hydroxide ligand in this crystal structure are 2.144(3) (Re_1–OH) and 2.134(2) (Re_2–OH) Å, indicating that this interaction is relatively symmetric. The Re–C distances of the carbonyl ligands that are trans to the bridging hydroxide are 1.902(4) and 1.918(4) Å. Notably, these distances are not significantly different from other Re–C distances in the mononuclear structures, indicating that the bridging hydroxide does not give rise to a significant trans influence. Generally, these bond metrics are consistent with the previously reported bridging hydroxide complexes discussed above [39–43].

2.3. Photophysical properties

Modifications of the axial ligands of the diimine Re(CO)$_3$ complexes can substantially alter their photophysical properties, giving rise to photoreactive and highly luminescent compounds [1,2]. The appropriate tuning of these properties can render these complexes useful for biological applications, such as imaging [10–13]. The photophysical properties of **Re-pip**, **Re-morph**, **Re-thio**, and **Re-py** in physiologically relevant air-equilibrated pH 7.4 phosphate-buffered saline (PBS) with less than 1% acetonitrile are reported in Table 2. All complexes exhibit similar absorbance profiles (Fig. 2) with peaks at 223 nm, 255 nm, 278 nm, 325 nm, and 367 nm. The higher energy bands (<325 nm) can reasonably be assigned to π–π* intraligand (IL) transitions, and the lower energy absorbance maximum at 367 nm arises from the excitation to the MLCT state [44–49]. Notably, the electronic absorbance spectra of these four compounds are effectively identical. This result indicates that the axial nitrogen donor ligands have a small effect on the IL and MLCT transitions. Because the MLCT arises from a transition of an electron in a metal d orbital with π symmetry (t_{2g} set) to the diimine π* ligand, the absence of a significant effect is consistent with the predominately σ-donor nature of these axial ligands.

Evaluation of the photoluminescence properties of these complexes reveals them to have modest emission quantum yields ranging from 1.66 to 3.09% (Table 2) under air-equilibrated aqueous conditions. Within this series, **Re-pip** has the lowest quantum yield, and **Re-py** has the highest. The energies of these emissions, which arise from relaxation of the ^{3}MLCT state, vary slightly among these complexes. **Re-py** has the highest energy ^{3}MLCT emission at 18,350 cm^{-1}, whereas **Re-pip** has the lowest energy ^{3}MLCT emission at 17,700 cm^{-1}. For **Re-morph** and **Re-thio**, these energies are effectively the same at 17,860 cm^{-1}. These results can be somewhat correlated to the basicity of the axial donor ligands. For example, py is the least basic (conjugate acid pK_a = 5.0) and gives rise to the Re complex with the highest quantum yield and emission energy, whereas pip is the most basic (conjugate acid pK_a = 11.2) and gives rise to the lowest quantum yield and emission energy. Morph and thio, which have similar basicities (conjugate acid pK_a = 8.4 and 9.0, respectively), also confer their Re(CO)$_3$ complexes with nearly identical emission properties that fall between those of **Re-py** and **Re-pip**. This trend relating basicity of axial donor ligands with

Table 2
Photophysical properties of rhenium complexes.

Compound	λ_{max}, nm (ε, $M^{-1}cm^{-1}$)	Φ_{lum}, % (λ_{max}, nm)[a]	τ (μs)[a]	τ (nitrogen, μs)[a,b]
Re-pip	225 (31300 ± 1300), 257 (18200 ± 800), 278 (22100 ± 900), 326 (5100 ± 200), 368 (3500 ± 100)	1.66 ± 0.06 (565)	0.31	0.49
Re-morph	224 (30700 ± 1900), 256 (17700 ± 1300), 278 (22400 ± 1600), 325 (5300 ± 400), 368 (3400 ± 200)	2.14 ± 0.16 (560)	0.52	0.70
Re-thio	222 (32300 ± 1000), 257 (18400 ± 600), 278 (23300 ± 800), 325 (5600 ± 200), 367 (3700 ± 30)	2.38 ± 0.31 (560)	0.47	0.97
Re-py	223 (35300 ± 600), 254 (22800 ± 400), 277 (28300 ± 600), 325 (6400 ± 100), 367 (3900 ± 100)	3.09 ± 0.30 (545)	0.62	1.00

[a] λ_{ex} = 350 nm.
[b] Luminescence lifetime measured in nitrogen-saturated pH 7.4 PBS.

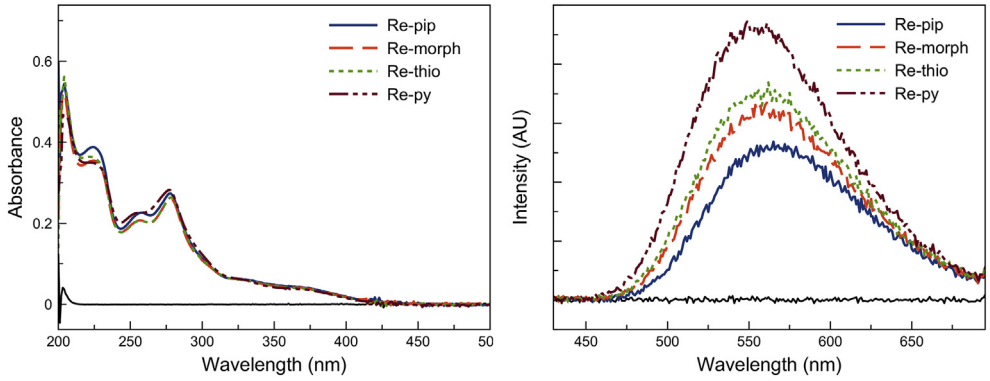

Fig. 2. UV–vis (left) and emission (right) spectra of **Re-pip** (blue), **Re-morph** (red), **Re-thio** (green), and **Re-py** (purple) in PBS with <1% acetonitrile at 25 °C (10 μM). (For interpretation of the references to colour in this figure legend, the reader is referred to the Web version of this article.)

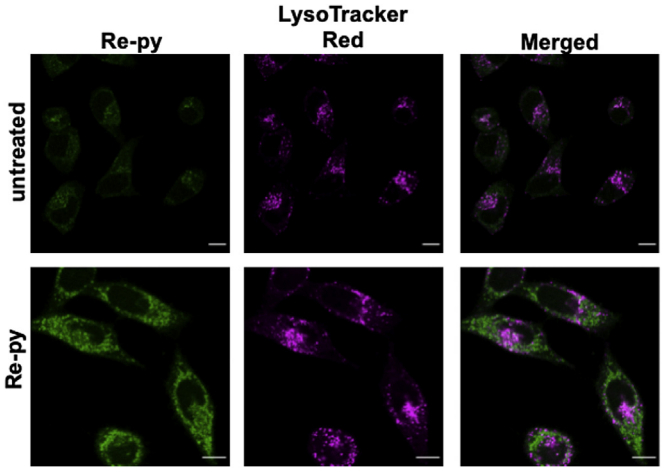

Fig. 3. Confocal fluorescence microscopy images of HeLa cells untreated or treated with **Re-py** (100 μM) and LysoTracker Red for 2 h (scale bar = 10 μm). (For interpretation of the references to colour in this figure legend, the reader is referred to the Web version of this article.)

^{3}MLCT emission energy has previously been reported [31]. The greater effect of the axial ligand on the ^{3}MLCT excited state and not on the ^{1}MLCT ground state would indicate that the axial nitrogen-donor ligand is contributing more to the triplet excited state.

The excited state lifetimes were also determined for these complexes in air-equilibrated and deoxygenated PBS (Table 2). Lifetimes for all complexes range from 0.3 to 0.6 μs, under ambient conditions (Figs. S18–S21). In the absence of oxygen, these lifetimes are approximately twice as long (Figs. S18–S21). This result is consistent with the known sensitivity of the ^{3}MLCT state of $Re(CO)_3$ complexes to quenching by oxygen [50].

2.4. Biological properties

To assess the suitability of these complexes for biological applications, we carried out confocal fluorescence microscopy studies using HeLa cervical cancer cells. The HeLa cells were treated with 100 μM of the compounds for 2 h prior to imaging. Of these four compounds, only **Re-py** gave rise to an emission intensity that was distinguishable from the background autofluorescence in the cells. Based on colocalization studies using LysoTracker Red and MitoTracker Red, **Re-py** appears to not significantly accumulate in either

the lysosomes or the mitochondria (Fig. 3 and S22). Its localization is mostly in the cytosol. Fluorescence microscopy imaging studies of A549 lung cancer cells treated with 200 μM of **Re-py** for 2 h were previously investigated [17]. In this prior study, however, no significant intracellular luminescence from this compound was detected. This discrepancy with the present work most likely arises from the use of different cell lines. Thus, the cellular uptake and intracellular luminescence of these $Re(CO)_3$ complexes may be highly dependent on the type of cells investigated. It is noteworthy that, despite the similar emission quantum yields of the four complexes measured in a cuvette, only **Re-py** could effectively be imaged in cells. The failure of **Re-pip**, **Re-morph**, and **Re-thio** for use in this application could arise in part due to poorer accumulation of these compounds in cells. Additionally, it has been noted that the photoluminescence properties of $Re(CO)_3$ complexes are sensitive to their local environments [51–54]. As such, the uptake and intracellular localization of these compounds may not be accurately reflected by fluorescence microscopy measurements. Non-environment sensitive methods like inductively-coupled plasma mass spectrometry or optical emission spectroscopy can provide a more accurate assessment of the complex uptake.

Given the reported anticancer activity of related $Re(CO)_3$ complexes [3–7], we evaluated the in vitro cytotoxicity of **Re-pip**, **Re-morph**, **Re-thio**, and **Re-py** in HeLa cells by the 3-(4,5-dimethylthiazol-2-yl)-2,5-tetrazolium bromide (MTT) assay. The resulting dose-response curves are shown in Fig. 4 and the 50% growth inhibitory concentration (IC_{50}) values are collected in Table 3. Among these four complexes, **Re-pip** and **Re-morph** are not active at concentrations below 100 μM. **Re-py** and **Re-thio** exhibit modest activity as characterized by IC_{50} values of 51 and 36 μM, respectively. Thus, these complexes are significantly less active than the clinically approved metal-based drug cisplatin, which exhibits an IC_{50} value of 6.6 μM in HeLa cells, and other $Re(CO)_3$ complexes explored in our lab with IC_{50} values of less than 10 μM [55–58]. The low activity of these complexes may be related to their low intracellular luminescence, which may suggest that they are poorly taken up by cells.

3. Conclusions

In this study, we have prepared a small set of $Re(CO)_3$ diimine complexes with axial nitrogen-donor ligands of differing basicity and evaluated their biological properties. For this class of compounds, the axial ligand appears to have only a minor influence on the photophysical properties of these complexes. This minimal effect may be a consequence of the σ-donor properties of the ligands evaluated, which interact poorly with the π symmetry metal d orbitals that modulate the photophysical properties of these complexes. Furthermore, the imaging properties and cytotoxic activities of these complexes are poor in comparison to other $Re(CO)_3$ complexes that have been evaluated for similar applications [3–9]. These results suggest that alterations to the axial ligand, involving the use of different donor atoms or ligand types, would be a more promising avenue for achieving complexes with greater biological relevance. Alternatively, a number of $Re(CO)_3$ complexes bearing py-based axial ligands have found use as imaging and cytotoxic agents [18–30]. In these cases, more dramatic alterations of the py ligand, with targeting groups for example, were able to achieve these successful results. The combination of the subtle changes of axial ligand donor strength, as evaluated in this study, with ligands that are tuned specifically for targeting or enhanced biological activity may yield new interesting $Re(CO)_3$ complexes for probing cellular systems. Although increasing the donor strength of the axial ligand decreases the emissive properties of the complex, this characteristic appears not to directly correlate with the cytotoxicity of the complexes. This result indicates that donor strength of the ligands surrounding the metal center may not be the key driver for the anticancer activity of this class of compounds and that other factors, such as ligand lipophilicity, may have more profound influences on their biological activities.

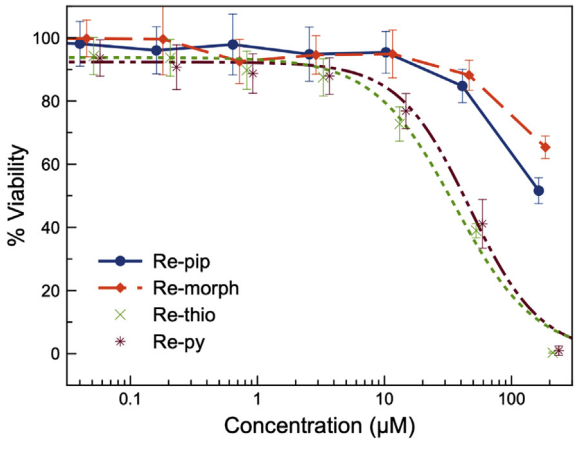

Fig. 4. Dose-response curves of **Re-pip** (blue circles), **Re-morph** (red diamonds), **Re-thio** (green crosses), and **Re-py** (purple stars) in HeLa cells. (For interpretation of the references to colour in this figure legend, the reader is referred to the Web version of this article.)

Table 3
IC_{50} values of rhenium complexes and cisplatin in HeLa cells.

Compound	IC_{50} (μM)
Re-pip	>164
Re-morph	>185
Re-thio	36 ± 3
Re-py	51 ± 5
cisplatin	6.6 ± 0.7

4. Experimental

4.1. Methods and materials

Rhenium carbonyl was purchased from Pressure Chemicals (Pittsburgh, Pennsylvania, USA). The ligand 1,10-phenanthroline (phen) was purchased from Sigma Aldrich (St. Louis, Missouri, USA) and was used as received. $Re(CO)_5Cl$ [58] and *fac*-[$Re(CO)_3$(phen)Cl] [59,60] were synthesized as previously described. All solvents were ACS grade or higher. All reactions were carried out under ambient atmospheric conditions without any effort to exclude water or oxygen.

4.2. Physical measurements

NMR samples were prepared as solutions using MeOH-d_4 or DMSO-d_6 as a solvent. NMR spectra were acquired on a Varian Inova 400 MHz spectrometer. ^1H NMR chemical shifts were referenced to residual solvent peaks versus tetramethylsilane (TMS) at 0 ppm. ^{19}F NMR spectra were referenced using an external standard of KPF_6 in D_2O (^{19}F $\delta = -72$ ppm vs $CFCl_3$ at 0 ppm). Samples for IR spectroscopy were prepared as KBr pellets and were analyzed on a Nicolet Avatar 370 DTGS (ThermoFisher Scientific, Waltham, MA). Analytical HPLC was carried out on a LC-20AT pump with a SPD-20AV UV–vis detector monitored at 270 and 220 nm (Shimadzu, Japan) using an Ultra Aqueous C18 column (100 Å, 5 μm,

250 mm × 4.6 mm, Restek, Bellefonte, PA) at a flow rate of 1 ml/min with a mobile phase containing 0.1% trifluoroacetic acid (TFA) in H_2O or MeOH. The method consisted of 5 min at 10% MeOH, followed by a linear gradient to 100% MeOH over 20 min. High-resolution mass spectra (HRMS) were recorded on an Exactive Orbitrap mass spectrometer in positive ESI mode (ThermoFisher Scientific, Waltham, MA) with samples injected as acetonitrile/water solutions with 1% formic acid. Elemental analyses (C, H, N) were performed by Atlantic Microlab Inc. (Norcross, Georgia, USA). UV−visible spectra were recorded on a Cary 8454 UV−vis (Agilent Technologies, Santa Clara, CA) or a Beckman Coulter DU800 UV−vis using 1-cm quartz cuvettes. Lifetime measurements were collected as described below. Luminescence quantum yield measurements were carried out on a Beckman Coulter DU800 UV−vis and Varian Eclipse Fluorometer.

4.3. X-ray crystallography

X-ray quality crystals of the complexes were grown by vapor diffusion of diethyl ether into acetonitrile or THF solutions of the complex. Low temperature X-ray diffraction (100 K) data was collected on a Rigaku XtaLAB Synergy diffractometer equipped with a 4-circle Kappa goniometer and HyPix 6000HE Hybrid Photon Counting (HPC) detector with monochromated Mo Kα radiation (λ = 0.7107 Å). Diffraction images were processed using the CrysAlisPro [61] software. The structure was solved through intrinsic phasing using SHELXT [62] and refined against F^2 on all data by full-matrix least-squares with SHELXL [63,64] following established strategies [65]. All non-hydrogen atoms were refined anisotropically. Hydrogen atoms bound to heteroatoms were located in the Fourier difference map and subsequently refined semifreely with the help of distance restraints. The isotropic displacement parameters of all hydrogen atoms were fixed to 1.2 times (1.5 times for methyl groups) the Ueq value of the atoms that they are linked to. Crystallographic data collection and refinement parameters are given in Table S1.

4.4. Emission quantum yield

The luminescence quantum yields were measured relative to the standard quinine sulfate (Φ = 0.52, 0.05 M H_2SO_4), which was cross-referenced in our lab to harmaline (Φ = 0.32, 0.05 M H_2SO_4) [66]. An excitation wavelength of 350 nm was used for the samples and standards. The compounds were measured as solutions in pH 7.4 PBS with <1% acetonitrile with the absorbance maintained below 0.1 to prevent inner filter effects [66]. At least five different concentrations of the samples and standards were measured by UV−vis and fluorescence spectroscopy, and the absorbance at 350 nm was plotted versus the integrated emission intensity. The slopes of the resulting lines were used in the equation:

$$\Phi_{sample} = \Phi_{ref}\frac{S_{sample}\eta^2_{sample}}{S_{ref}\eta^2_{ref}} \quad (1)$$

where Φ_{ref} is the quantum yield of the reference, quinine sulfate, and S is the slope of either the sample or the reference, and η is the refractive index of the solvent.

4.5. Lifetime measurements

Laser excitation for the phosphorescence lifetime measurements was provided by pulsing the 405 nm laser line from a four-line iChrome MLE laser (Toptica Photonics AG, Munich, Germany). The diode laser in the iChrome was triggered by a DG535 Digital Delay/Pulse Generator (Stanford Research, Sunnyvale, CA) at 100 KHz and delivered 100 ns FWHM 405 nm excitation pulses. The 405 nm pulses were fiber-delivered to a sample-filled cuvette and phosphorescence was collected at 90° to a Bialkali photomultiplier tube (HC125, Hamamatsu, Bridgewater, NJ) through a 470 nm long pass filter (HQ470lp, Chroma Technology, Bellows Falls, VT). The time-resolved photon counts were collected in 40 ns time bins using a SR430 Multi-channel scaler (Stanford Research, Sunnyvale, CA). Data was transferred to a PC via the SR430 GPIB bus and fit to the standard exponential decay model using MagicPlot Pro software. Measurements were collected in PBS solutions at 30−50 nM. For deoxygenated measurements, nitrogen gas was bubbled into the PBS solutions for 30 min and then the lifetime was determined.

4.6. Synthetic procedures

4.6.1. Synthesis of fac-[Re(CO)$_3$(phen)(piperidine)]OTf (**Re-pip**)

A mixture of [Re(CO)$_3$(phen)Cl] (0.200 g, 0.42 mmol) and AgOTf (0.106 g, 0.42 mmol) in THF (48 ml) was heated to reflux for 3 h in the dark. The white solid AgCl was removed via vacuum filtration. To the remaining yellow filtrate, piperidine (0.183 g, 2.1 mmol) was added, and the resulting solution was heated to reflux for an additional 24 h. The reaction mixture was allowed to cool to room temperature, concentrated to about 5−10 ml, and then placed in a −20 °C freezer overnight. The yellow crystals that formed were then filtered and washed with THF. The crude product was purified by recrystallizing twice by allowing a concentrated solution of the compound in THF (2−4 ml) to slowly evaporate at room temperature. Yield: 0.050 g (17%). ^{1}H NMR (400 MHz, MeOH-d_4): δ 9.51 (d, 2H), 9.09 (d, 2H), 8.41 (s, 2H), 8.20 (dd, 2H), 4.25 (t, 1H), 2.89 (d, 2H), 2.69 (m, 2H), 1.50 (m, 1H), 1.36 (m, 3H), 1.15 (m, 2H). ^{19}F NMR (376 MHz, MeOH-d_4, external stnd: KPF_6): 77.08. IR (KBr, cm^{-1}): 2025 s, 1932 s, 1893 s. ESI-MS (pos. ion mode, CH_3CN:H_2O 70:30 and 1% formic acid): 536.0945 *m/z* ([M]$^+$, calcd. 536.0984). Anal. Calcd. for $C_{21}H_{19}F_3N_3O_6ReS$: C, 36.84; H, 2.80; N, 6.14. Found: C, 36.66; H, 2.80; N, 6.12.

4.6.2. Synthesis of fac-[Re(CO)$_3$(phen)(morpholine)]OTf (**Re-morph**)

A mixture of *fac*-[Re(CO)$_3$(phen)Cl] (0.200 g, 0.42 mmol) and AgOTf (0.106 g, 0.42 mmol) in THF (48 ml) was heated to reflux for 3 h in the dark. The white solid AgCl was removed via vacuum filtration. To the remaining yellow filtrate, morpholine (0.183 g, 2.1 mmol) was added, and the resulting solution was heated to reflux for an additional 24 h. The reaction mixture was allowed to cool to room temperature, and yellow precipitate formed, which was filtered and washed with cold THF (~20 ml). Yield: 0.134 g (47%). ^{1}H NMR (400 MHz, MeOH-d_4): δ 9.52 (d, 2H), 9.10 (d, 2H), 8.41 (s, 2H), 8.21 (dd, 2H), 4.83 (t, 1H), 3.46 (d, 2H), 3.19 (t, 2H), 2.81 (m, 2H), 2.64 (d, 2H). ^{19}F NMR (376 MHz, MeOH-d_4, external stnd: KPF_6): 77.08. IR (KBr, cm^{-1}): 2033 s, 1940 s, 1919 s, 1903 s. ESI-MS (pos. ion mode, CH_3CN:H_2O 70:30 and 1% formic acid): 538.0739 *m/z* ([M]$^+$, calcd. 538.0777). Anal. Calcd. for $C_{20}H_{17}F_3N_3O_7ReS$: C, 34.99; H, 2.50; N, 6.12. Found: C, 35.07; H, 2.46; N, 6.05.

4.6.3. Synthesis of fac-[Re(CO)$_3$(phen)(thiomorpholine)]OTf (**Re-thio**)

A mixture of *fac*-[Re(CO)$_3$(phen)Cl] (0.241 g, 0.50 mmol) and AgOTf (0.127 g, 0.50 mmol) in THF (52 ml) was heated to reflux for 3 h in the dark. The white solid AgCl was removed via vacuum filtration. To the remaining yellow filtrate, thiomorpholine (0.258 g, 2.5 mmol) was added, and the resulting solution was heated to reflux for an additional 24 h. The reaction mixture was allowed to cool to room temperature and THF was removed by rotary

evaporation. The dark yellow solid was then taken up in 65 °C THF (3–5 ml). The hot solution was stored at −20 °C, inducing the precipitation of a yellow solid. The yellow precipitate was filtered and washed with cold THF. Yield: 0.067 g (19%). ^{1}H NMR (400 MHz, MeOH-d_4): δ 9.52 (d, 2H), 9.11 (d, 2H), 8.43 (d, 2H), 8.31 (dd, 2H), 4.58 (t, 1H), 3.20 (d, 2H), 2.90 (m, 2H), 2.45 (m, 2H), 2.26 (d, 2H). ^{19}F NMR (376 MHz, MeOH-d_4, external stnd: KPF_6): 77.08. IR (KBr, cm^{-1}): 2027 s, 1930 s, 1896 s. ESI-MS (pos. ion mode, CH_3CN:H_2O 70:30 and 1% formic acid): 554.0513 *m/z* ($[M]^+$, calcd. 554.0548). Anal. Calcd. for $C_{20}H_{17}F_3N_3O_6ReS_2$: C, 34.19; H, 2.44; N, 5.98. Found: C, 34.40; H, 2.34; N, 6.15.

4.6.4. Synthesis of *fac*-[Re(CO)$_3$(phen)(pyridine)]OTf (***Re-py***)

fac-$[Re(CO)_3(phen)(pyridine)]^+$ was synthesized as previously described [17,31]. ^{1}H NMR (400 MHz, DMSO-d_6): δ 9.77 (d, 2H), 9.04 (d, 2H), 8.46 (d, 2H), 8.31 (s, 2H), 8.26 (dd, 2H), 7.86 (t, 1H), 7.32 (t, 2H). ^{19}F NMR (376 MHz, DMSO-d_6, external stnd: KPF_6): 77.04. IR (KBr, cm^{-1}): 2027 s, 1928 sh, 1911 s.

4.7. Cell culture and cytotoxicity

HeLa (cervical cancer) cell line was obtained from American Type Culture Collection (ATCC) and cultured using Dulbecco's Modified Eagle's Medium (DMEM) supplemented with 10% fetal bovine serum (FBS). The cell line was grown in a humidified incubator at 37 °C with an atmosphere of 5% CO_2. Cells were passed at 80–90% confluence using trypsin/EDTA. Cells were tested monthly for mycoplasma contamination with the PlasmoTest™ mycoplasma detection kit from InvivoGen.

All compounds were dissolved in DMSO to prepare a 10–20 mM stock solution, which was diluted in growth media to contain <1% DMSO. Cells were grown to 80–90% confluence, detached with trypsin/EDTA, seeded in 96-well plates at 4000 cells/well in 100 μL of growth media, and incubated for 24 h. The medium was removed and replaced with fresh medium (200 μL) containing varying concentrations of the desired compound or media. The cells were then incubated for an additional 48 h. The medium was removed from the wells, and MTT in DMEM (200 μL, 1 mg/ml) was added. The additional 48 h incubation was performed to ensure that the cells were in the logarithmic growth phase and that the cells had adequate time to regrow after exposure to the complexes. After 4 h, the MTT/DMEM solution was removed, and the formazan crystals were dissolved in 200 μL of an 8:1 mixture of DMSO and pH 10 glycine buffer. The absorbance at 570 nm in each well was measured using a BioTek Synergy HT plate reader. Cell viability was determined by normalizing the absorbance of the treated wells to untreated wells. The concentrations of the compounds versus % viability were plotted to produce the dose-response curves, which were analyzed using a logistic sigmoid function fit with MagicPlot Pro software. The reported IC_{50} values are the average of at least three independent experiments with six replicates per concentration level.

4.8. Colocalization using confocal fluorescence microscopy

A total of 1×10^5 HeLa cells were seeded onto 35 mm glass bottom dishes. After 24 h, the cells were treated with the rhenium compounds (100 μM) for 2 h or the specific dye for 30 min in DMEM media. After the indicated time, the media was removed and the cells were washed with PBS and fresh media was added. Right before imaging, the media was removed and imaging buffer was added (20 mM HEPES pH 7.4, 135 mM NaCl, 5 mM KCl, 1.8 mM $CaCl_2$, 1 mM $MgCl_2$, 1 mg/mL glucose, and 1 mg/mL bovine serum albumin). The cells were imaged with a Zeiss LSM 800 or Zeiss LSM 880 confocal laser-scanning microscope. The rhenium complex was imaged using a 405 nm laser excitation with a 410–550 nm emission filter and images were processed using ImageJ software. For MitoTracker Red and LysoTracker Red DND-99 treatment, 1 μL of 100 μM dye was added to 3 mL of medium 30 min prior to imaging and the dyes were excited with a 561 nm laser with an emission filter from 630 to 700 nm.

Accession codes

CCDC 1965772–1965776 contains the supplementary crystallographic data for this paper. These data can be obtained free of charge via www.ccdc.cam.ac.uk/data_request/cif, or by emailing data_request@ccdc.cam.ac.uk, or by contacting The Cambridge Crystallographic Data Center, 12 Union Road, Cambridge CB2 1EZ, UK; fax: +44 1223 336033.

Declaration of competing interest

The authors declare that they have no known competing financial interests or personal relationships that could have appeared to influence the work reported in this paper.

Acknowledgements

This research was supported by Cornell University and by the Office of the Assistant Secretary of Defense for Health Affairs through the Ovarian Cancer Research Program under award no. W81XWH-17-1-0097. This work made use of the NMR facility at Cornell University, which is supported, in part, by the NSF under award number CHE-1531632. We thank Prof. Jeremy Baskin and Prof. Warren Zipfel for allowing us to use their confocal fluorescence microscope and assistance with fluorescence decay lifetime measurements, respectively.

Appendix A. Supplementary data

Supplementary data to this article can be found online at https://doi.org/10.1016/j.jorganchem.2019.121064.

References

[1] A. Kumar, S.-S. Sun, A.J. Lees, Photophysics and photochemsitry of organometallic rhenium diimine complexes, in: A.J. Lees (Ed.), Photophysics of Organometallics, Springer, Berlin, Heidelberg, 2010, pp. 1–36, https://doi.org/10.1007/978-3-642-04729-9.
[2] R.A. Kirgan, B.P. Sullivan, D.P. Rillema, Photochemistry and photophysics of coordination compounds: rhenium, in: Photochem. Photophysics Coord. Compd. II, 2007, pp. 45–100, https://doi.org/10.1007/978-3-540-73349-2.
[3] C.C. Konkankit, S.C. Marker, K.M. Knopf, J.J. Wilson, Dalton Trans. 47 (2018) 9934–9974, https://doi.org/10.1039/c8dt01858h.
[4] P. Collery, D. Desmaele, V. Veena, Curr. Pharmaceut. Des. 25 (2019) 1–17, https://doi.org/10.2174/1381612825666190902161400.
[5] E.B. Bauer, A.A. Haase, R.M. Reich, D.C. Crans, F.E. Kühn, Coord. Chem. Rev. 393 (2019) 79–117, https://doi.org/10.1016/j.ccr.2019.04.014.
[6] A. Leonidova, G. Gasser, ACS Chem. Biol. 9 (2014) 2180–2193, https://doi.org/10.1021/cb500528c.
[7] L.C.-C. Lee, K.-K. Leung, K.K.-W. Lo, Dalton Trans. 46 (2017) 16357–16380, https://doi.org/10.1039/c7dt03465b.
[8] C. Otero, A. Carreño, R. Polanco, F.M. Llancalahuen, R. Arratia-Pérez, M. Gacitúa, J.A. Fuentes, Front. Chem. 7 (2019) 1–12, https://doi.org/10.3389/fchem.2019.00454.
[9] S. Hostachy, C. Policar, N. Delsuc, Coord. Chem. Rev. 351 (2017) 172–188, https://doi.org/10.1016/j.ccr.2017.05.004.
[10] K.K.-W. Lo, A.W.-T. Choi, W.H.-T. Law, Dalton Trans. 41 (2012) 6021–6047, https://doi.org/10.1039/c2dt11892k.
[11] K.K.-W. Lo, Acc. Chem. Res. 48 (2015) 2985–2995, https://doi.org/10.1021/acs.accounts.5b00211.
[12] V. Fernández-Moreira, F.L. Thorp-Greenwood, M.P. Coogan, Chem. Commun. 46 (2010) 186–202, https://doi.org/10.1039/B917757D.
[13] Q. Zhao, C. Huang, F. Li, Chem. Soc. Rev. 40 (2011) 2508–2524, https://doi.org/10.1039/c0cs00114g.
[14] M. Schutte, G. Kemp, H.G. Visser, A. Roodt, Inorg. Chem. 50 (2011)

12486–12498, https://doi.org/10.1021/ic2013792.
[15] K. Koike, N. Okoshi, H. Hori, K. Takeuchi, O. Ishitani, H. Tsubaki, I.P. Clark, M.W. George, F.P.A. Johnson, J.J. Turner, J. Am. Chem. Soc. 124 (2002) 11448–11455, https://doi.org/10.1021/ja017032m.
[16] K. Koike, J. Tanabe, S. Toyama, H. Tsubaki, K. Sakamoto, J.R. Westwell, F.P.A. Johnson, H. Hori, H. Saitoh, O. Ishitani, Inorg. Chem. 39 (2000) 2777–2783, https://doi.org/10.1021/ic991190l.
[17] J. Yang, J.-X. Zhao, Q. Cao, L. Hao, D. Zhou, Z. Gan, L.-N. Ji, Z.-W. Mao, ACS Appl. Mater. Interfaces 9 (2017) 13900–13912, https://doi.org/10.1021/acsami.7b01764.
[18] M.-W. Louie, A.W.-T. Choi, H.-W. Liu, B.T.-N. Chan, K.K.-W. Lo, Organometallics 31 (2012) 5844–5855, https://doi.org/10.1021/om3003575.
[19] R.-R. Ye, C.-P. Tan, Y.-N. Lin, L.-N. Ji, Z.-W. Mao, Chem. Commun. 51 (2015) 8353–8356, https://doi.org/10.1039/c5cc02354h.
[20] A.J. Amoroso, M.P. Coogan, J.E. Dunne, V. Fernández-Moreira, J.B. Hess, A.J. Hayes, D. Lloyd, C. Millet, S.J.A. Pope, C. Williams, Chem. Commun. (2007) 3066–3068, https://doi.org/10.1039/b706657k.
[21] A.W.-T. Choi, M.-W. Louie, S.P.-Y. Li, H.-W. Liu, B.T.-N. Chan, T.C.-Y. Lam, A.C.-C. Lin, S.-H. Cheng, K.K.-W. Lo, Inorg. Chem. 51 (2012) 13289–13302, https://doi.org/10.1021/ic301948d.
[22] M.-W. Louie, H.-W. Liu, M.H.-C. Lam, T.-C. Lau, K.K.-W. Lo, Organometallics 28 (2009) 4297–4307, https://doi.org/10.1021/om900311s.
[23] K.K.-W. Lo, M.-W. Louie, K.-S. Sze, J.S.-Y. Lau, Inorg. Chem. 47 (2008) 602–611, https://doi.org/10.1021/ic701675c.
[24] K.Y. Zhang, K.K.-S. Tso, M.-W. Louie, H.-W. Liu, K.K.-W. Lo, Organometallics 32 (2013) 5098–5102, https://doi.org/10.1021/om400612f.
[25] M.-W. Louie, H.-W. Liu, M.H.-C. Lam, Y.-W. Lam, K.K.-W. Lo, Chem. Eur J. 17 (2011) 8304–8308, https://doi.org/10.1002/chem.201101399.
[26] M.-W. Louie, T.T.-H. Fong, K.K.-W. Lo, Inorg. Chem. 50 (2011) 9465–9471, https://doi.org/10.1021/ic201143f.
[27] J. Yang, Q. Cao, H. Zhang, L. Hao, D. Zhou, Z. Gan, Z. Li, Y.-X. Tong, L.-N. Ji, Z.-W. Mao, Biomaterials 176 (2018) 94–105, https://doi.org/10.1016/j.biomaterials.2018.05.040.
[28] A. Leonidova, V. Pierroz, L.A. Adams, N. Barlow, S. Ferrari, B. Graham, G. Gasser, ACS Med. Chem. Lett. 5 (2014) 809–814, https://doi.org/10.1021/ml500158w.
[29] A.W.-T. Choi, K.K.-S. Tso, V.M.-W. Yim, H.-W. Liu, K.K.-W. Lo, Chem. Commun. 51 (2015) 3442–3445, https://doi.org/10.1039/c4cc09532d.
[30] V. Fernández-Moreira, F.L. Thorp-Greenwood, A.J. Amoroso, J. Cable, J.B. Court, V. Gray, A.J. Hayes, R.L. Jenkins, B.M. Kariuki, D. Lloyd, C.O. Millet, C.F. Williams, M.P. Coogan, Org. Biomol. Chem. 8 (2010) 3888–3901, https://doi.org/10.1039/c004610h.
[31] S.M. Fredericks, J.C. Luong, M.S. Wrighton, J. Am. Chem. Soc. 101 (1979) 7415–7417, https://doi.org/10.1021/ja00518a054.
[32] M. Rubiralta, E. Giralt, A. Diez, Conformational analysis of piperidine, in: Piperidine Structure, Preparation, Reactivity, and Synthetic Applications of Piperidine and Its Derivatives, Elsevier, 1991, pp. 24–33.
[33] R.K. Harris, R.A. Spragg, J. Chem. Soc. B (1968) 684–691, https://doi.org/10.1039/J29680000684.
[34] R.K. Harris, R.A. Spragg, Chem. Commun. (1966) 314–316, https://doi.org/10.1039/C19660000314.
[35] D.C. Harris, M.D. Bertolucci, Symmetry and spectroscopy: An introduction to vibrational and electronic spectroscopy, Dover Publications, Inc., New York, NY, 1978.
[36] J.J. Turner, F.-W. Grevels, S.M. Howdle, J. Jacket, M.T. Haward, W.E. Klotzbücher, J. Am. Chem. Soc. 113 (1991) 8347–8353, https://doi.org/10.1021/ja00022a022.
[37] F.-W. Grevels, K. Kerpen, W.E. Klotzbucher, R.E.D. McClung, G. Russell, M. Voitte, K. Schaffner, J. Am. Chem. Soc. 120 (1998) 10423–10433, https://doi.org/10.1021/ja973897h.
[38] M.C. Zoerb, J.S. Henderson, S.D. Glover, J.P. Lomont, S.C. Nguyen, A.D. Hill, C.P. Kubiak, C.B. Harris, J. Phys. Chem. B 119 (2015) 10738–10749, https://doi.org/10.1021/acs.jpcb.5b06734.
[39] P.J. Heard, P. Sroisuwan, D.A. Tocher, Polyhedron 22 (2003) 1321–1327, https://doi.org/10.1016/S0277-5387(03)00102-5.
[40] L. Cuesta, D.C. Gerbino, E. Hevia, D. Morales, M.E.N. Clemente, J. Perez, L. Riera, V. Riera, D. Miguel, I. del Rio, S. Garcìa-Granda, Chem. Eur J. 10 (2004) 1765–1777, https://doi.org/10.1002/chem.200305577.
[41] D.H. Gibson, M.S. Mashuta, X. Yin, Acta Crystallogr. Sect. E. E59 (2003) m911–m913, https://doi.org/10.1107/S1600536803020105.
[42] K. Ruth, T. Morawitz, H.-W. Lerner, M. Bolte, Acta Crystallogr. Sect. E. E64 (2008) m496, https://doi.org/10.1107/S160053680800490X.
[43] C. Muñoz, M. Saldías, P. Oyarzún, J.-Y. Saillard, J.-R. Hamon, G. Calvez, N. Pizarro, A. Vega, Polyhedron 173 (2019) 114150, https://doi.org/10.1016/j.poly.2019.114150.
[44] P.J. Giordano, M.S. Wrighton, J. Am. Chem. Soc. 101 (1979) 2888–2897, https://doi.org/10.1021/ja00505a016.
[45] G. Tapolsky, R. Duesing, T.J. Meyer, Inorg. Chem. 29 (1990) 2285–2297, https://doi.org/10.1021/ic00337a021.
[46] L.A. Worl, R. Duesing, P. Chen, L.D. Ciana, T.J. Meyer, J. Chem. Soc., Dalton Trans. (1991) 849–858, https://doi.org/10.1039/dt9910000849.
[47] L. Wallace, D.P. Rillema, Inorg. Chem. 32 (1993) 3836–3843, https://doi.org/10.1021/ic00070a012.
[48] L.D. Ramos, H.M. da Cruz, K.P.M. Frin, Photochem. Photobiol. Sci. 16 (2017) 459–466, https://doi.org/10.1039/C6PP00364H.
[49] L. Sacksteder, A.P. Zipp, E.A. Brown, J. Streich, J.N. Demás, B.A. Degraff, Inorg. Chem. 29 (1990) 4335–4340, https://doi.org/10.1021/ic00346a033.
[50] M. Wrighton, D.L. Morse, J. Am. Chem. Soc. 96 (1974) 998–1003, https://doi.org/10.1021/ja00811a008.
[51] C.C. Konkankit, A.P. King, K.M. Knopf, T.L. Southard, J.J. Wilson, ACS Med. Chem. Lett. 10 (2019) 822–827, https://doi.org/10.1021/acsmedchemlett.9b00128.
[52] S. Imstepf, V. Pierroz, R. Rubbiani, M. Felber, T. Fox, G. Gasser, R. Alberto, Angew. Chem. Int. Ed. 55 (2016) 2792–2795, https://doi.org/10.1002/anie.201511432.
[53] S. Imstepf, V. Pierroz, P. Raposinho, M. Bauwens, M. Felber, T. Fox, A.B. Shapiro, R. Freudenberg, C. Fernandes, S. Gama, G. Gasser, F. Motthagy, I.R. Santos, R. Alberto, Bioconjug. Chem. 26 (2015) 2397–2407, https://doi.org/10.1021/acs.bioconjchem.5b00466.
[54] G. Gasser, S. Neumann, I. Ott, M. Seitz, R. Heumann, N. Metzler-Nolte, Eur. J. Inorg. Chem. (2011) 5471–5478, https://doi.org/10.1002/ejic.201100734.
[55] K.M. Knopf, B.L. Murphy, S.N. MacMillan, J.M. Baskin, M.P. Barr, E. Boros, J.J. Wilson, J. Am. Chem. Soc. 139 (2017) 14302–14314, https://doi.org/10.1021/jacs.7b08640.
[56] C.C. Konkankit, B.A. Vaughn, S.N. MacMillan, E. Boros, J.J. Wilson, Inorg. Chem. 58 (2019) 3895–3909, https://doi.org/10.1021/acs.inorgchem.8b03552.
[57] A.P. King, S.C. Marker, R.V. Swanda, J.J. Woods, S.-B. Qian, J.J. Wilson, Chem. Eur J. 25 (2019) 9206–9210, https://doi.org/10.1002/chem.201902223.
[58] S.C. Marker, S.N. MacMillan, W.R. Zipfel, Z. Li, P.C. Ford, J.J. Wilson, Inorg. Chem. 57 (2018) 1311–1331, https://doi.org/10.1021/acs.inorgchem.7b02747.
[59] P. Kurz, B. Probst, B. Spingler, R. Alberto, Eur. J. Inorg. Chem. (2006) 2966–2974, https://doi.org/10.1002/ejic.200600166.
[60] J.M. Smieja, C.P. Kubiak, Inorg. Chem. 49 (2010) 9283–9289, https://doi.org/10.1021/ic1008363.
[61] CrysAlisPro, in: CrysAlisPro, Rigaku OD Woodlands TX, CrysAlisPro, Rigaku OD, The Woodlands, TX, 2015.
[62] G.M. Sheldrick, Acta Crystallogr. Sect. A Found. Crystallogr. A71 (2015) 3–8, https://doi.org/10.1107/S2053273314026370.
[63] G.M. Sheldrick, Acta Crystallogr. Sect. C Cryst. Struct. Commun. C71 (2015) 3–8, https://doi.org/10.1107/S2053229614024218.
[64] G.M. Sheldrick, Acta Crystallogr. A: Found. Crystallogr. A64 (2008) 112–122, https://doi.org/10.1107/S0108767307043930.
[65] P. Müller, Crystallogr. Rev. 15 (2009) 57–83, https://doi.org/10.1080/08893110802547240.
[66] A.M. Brouwer, Pure Appl. Chem. 83 (2011) 2213–2228, https://doi.org/10.1351/PAC-REP-10-09-31.